Melting Behavior and Nonisothermal Crystallization Kinetics of Polyamide 6/Polyamide 66 Molecular Composites via *In Situ* Polymerization

Yulin Li,[1] Hongzhi Liu,[1] Ying Zhang,[2] Guisheng Yang[1,3]

[1]*Key Laboratory of Engineering Plastics, Joint Laboratory of Polymer Science and Materials, Institute of Chemistry, Chinese Academy of Sciences, Beijing 100080, People's Republic of China*
[2]*State Key Laboratory of Polymer Physics and Chemistry, Joint Laboratory of Polymer Science and Materials, Institute of Chemistry, Chinese Academy of Sciences, Beijing 100080, People's Republic of China*
[3]*Graduate School of the Chinese Academy of Sciences, Beijing 100080, People's Republic of China*

Received 10 August 2003; accepted 18 February 2005
DOI 10.1002/app.22392
Published online in Wiley InterScience (www.interscience.wiley.com).

ABSTRACT: The melting behavior and nonisothermal crystallization kinetics of pure polyamide 6 (PA 6) and its molecular composites with polyamide 66 (PA 66) were investigated with differential scanning calorimetry. The PA 6/PA 66 composites had one melting peak, whereas the coextruded PA 6/PA 66 blends had two melting peaks. With the addition of PA 66 to PA 6 via *in situ* anionic polymerization, the melting temperature, crystallization temperature, and crystallinity of PA 6 in the composites decreased. The half-time of nonisothermal crystallization increased for a PA 6/PA 66 molecular composite containing 12 wt % PA 66, in comparison with that of pure PA 6. The commonly used Ozawa equation was used to fit the nonisothermal crystallization of pure PA 6 and its composites. The Ozawa exponent values in the primary stage were equal to 1.28–3.03 and 1.28–2.97 for PA 6 and its composite with 12 wt % PA 66, respectively, and this revealed that the mechanism of primary crystallization of PA 6 and PA 6/PA 66 was mainly heterogeneous nucleation and growth. All the results indicated that the incorporation of PA 66 into PA 6 at the molecular level retarded the crystallization of PA 6. © 2005 Wiley Periodicals, Inc. J Appl Polym Sci 98: 2172–2177, 2005

Key words: composites; crystallization; polyamides

INTRODUCTION

It is well known that the physicomechanical properties of semicrystalline polymers, such as polyamides, are strongly influenced by the crystallinity and structure of the crystalline phase. The crystallization process affects the polymer properties through the crystalline structure and morphology established during the solidification process. An important aspect of the crystallization process is its kinetics, both from the fundamental view of polymer physics modeling and for the control of polymer processing operations. To obtain materials with better physical properties, it is important to study the nonisothermal crystallization kinetics because most practical processes, such as industrial synthesis, extrusion, molding, film forming, and melting spinning of synthetic fibers, frequently occur under situations close to nonisothermal conditions.[1] However, in comparison with pure semicrystalline materials, the crystalline microstructure and crystallization kinetics in polymer blends are not quite well understood.[2]

In our previous studies,[3] a series of novel polyamide 6 (PA 6) molecular composites with polyamide 66 (PA 66), PA 6/PA 66, were synthesized. The mechanical properties and morphology of the composites were studied. The mechanical data indicated that the mechanical properties of the composites were superior to those of pure PA 6, particularly as far as impact resistance was concerned. Unlike the apparent phase separation of the corresponding blend samples, the composites exhibited a more homogeneous morphology. A quite rough fracture surface for the composites was found in comparison with the smooth fracture in pure PA 6. The improvement in the toughness might be attributed to a decrease in the crystallinity of PA 6 and the special morphology found in the composites. The maintenance of the tensile strength could be ascribed to the special morphology in the composites. Because the crystallization behavior is very important for determining property profiles and end-use applications, the crystallization characteristics of this new family of PA 6/PA 66 composites have been studied in this work.

EXPERIMENTAL

Materials and preparation

PA 6 and its composites with PA 66 were prepared via the anionic ring-opening polymerization of ε-capro-

Correspondence to: G. Yang (ygs@Geniuscn.com).
Contract grant sponsor: 973 Program of the Ministry of Sciences and Technologies; contract grant number: 2003CB615602.

lactam with PA 66 dissolved in it, and the coextruded PA 6/PA 66 blends were prepared with a ϕ35 twin-screw extruder (SHJ-30) (Jiangsu Keya Chemical Engineer Co., Ltd., China) at a screw speed of 240 rpm and barrel temperatures of 230, 240, 245, 250, and 250°C. The preparation procedures are reported in detail in our previous article.[3] PA 6 composites with PA 66 and coextruded PA 6/PA 66 blends were denoted PA 6/PA 66 and e-PA 6/PA 66, respectively. The samples were kept *in vacuo* at 70°C for 8 h before the measurements.

UV spectrophotometry analysis

A PerkinElmer (Boston, MA) Lambda 9 UV spectrophotometer was used to monitor the presence of structural irregularities in PA 6 chains because they had strong absorption in the UV region.[4] The UV spectra were taken in 1% (w/w) solutions of the composite in anhydrous formic acid between 250 and 400 nm (path length = 1 cm); the optical density maximum at 270–280 nm was considered.

Viscosity measurements

The viscometric weight-average molecular weights (M_w's) of pure PA 6 and PA 6/PA 66 were determined by intrinsic viscosity ([η]) measurements (97% sulfuric acid) at a concentration of 0.2 g/dL with a suspended-level Ubbelohde viscometer (Sierkeda Instrument Co., Ltd., Shanghai, China) thermostated at 25.0 ± 0.1°C.

Differential scanning calorimetry (DSC) analysis

The melting behavior and nonisothermal crystallization kinetics were carried out on a PerkinElmer Pyris-1 differential scanning calorimeter with the temperature calibrated with indium. The melting behavior was determined as follows: all the DSC measurements were performed from room temperature to 270°C at a heating rate of 10°C/min under a nitrogen atmosphere, and the melting temperatures in the first scan and second scan (T_m and T_m', respectively) were determined.

The nonisothermal crystallization was performed as follows: the samples were heated at a certain heating rate to 250°C and held there for 10 min to eliminate residual crystals, and the melt was cooled to crystallize at different cooling rates (5, 10, 15, and 20°C/min) under a nitrogen atmosphere. The sample weights were 7–8 mg.

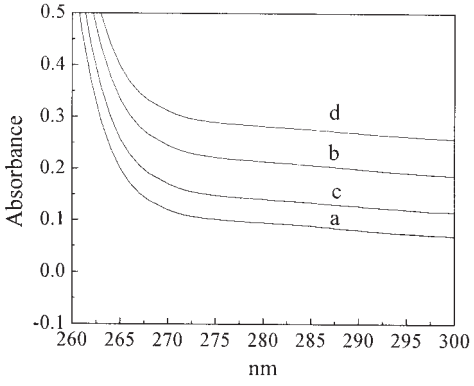

Figure 1 UV intensity profiles at the maximum (270–280 nm) for (a) formic acid, (b) pure PA 6, (c) PA 6/PA 66 (6 wt % PA 66), and (d) PA 6/PA 66 (12 wt % PA 66).

TABLE I
Effect of the PA 66 Content on the Molecular Weight of PA 6/PA 66

PA 66 (wt %)	[η] (dL/g)	$M_w \times 10^{-4}$
0	4.99	24.65
6	4.40	20.73
12	4.17	19.28
100[a]	1.32	4.09
PA 6 resin[a]	1.20	3.59

[a] Two polymers for the preparation of the blend sample.

RESULTS AND DISCUSSION

Molecular weight and chain regularity of pure PA 6 and PA 6/PA 66

An evaluation of the relevance and extent of side reactions, as a function of the PA 66 concentration, is shown in Figure 1. No absorption peak in the range of 250–400 nm was found for pure PA 6 and PA 6/PA 66. This reveals that the molecular chain of PA 6 is linear.[4]

M_w was estimated by [η] measurements with eq. (1):[5,6]

$$M_w = 2.81 \times 10^4[\eta]^{1.35} \quad (1)$$

Typical results are given in Table I. The calculations (see Table I) show that M_w slightly decreases with increasing PA 66 in PA 6/PA 66.

Melting behavior of pure PA 6, PA 6/PA 66, and Blends

Figure 2 shows the melting curves of PA 6/PA 66 and e-PA 6/PA 66 containing different PA 66 concentrations obtained from DSC measurements. A single endothermic peak of PA 6 can be observed for PA 6/PA 66, and the values of the single peak are below T_m of pure PA 6. However, separate endothermic peaks for both PA 6 and PA 66 can be observed for e-PA 6/PA 66. Because of the very rapid rate of the anionic polymerization of ε-caprolactam at a low polymerization temperature, amide interchange between two polyamides would not occur, so no random copolyamides would be formed.[7,8] With a slight increase in the PA 66

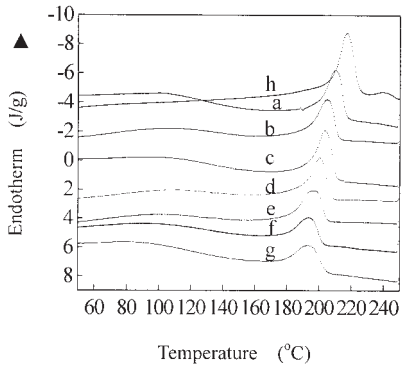

Figure 2 Second-run DSC melting curves of PA 6/PA 66 containing (a) 0 wt % PA 66, (b) 2 wt % PA 66, (c) 4 wt % PA 66, (d) 6 wt % PA 66, (e) 8 wt % PA 66, (f) 10 wt % PA 66, (g) 12 wt % PA 66, and (h) e-PA 6/PA 66 with 10 wt % PA 66.

concentration in PA 6/PA 66, T_m and the crystallinity of the PA 6 component in the composites decrease greatly (as shown later in Figs. 4 and 5). This indicates that the PA 66 macromolecular chains can be dispersed in the PA 6 matrix in the amorphous state. Because PA 6 and PA 66 are miscible in the amorphous state,[9] it can be concluded that the added PA 66 is not crystallized but dispersed in the PA 6 matrix at the molecular level.

Because of such large molecular weights, the effect of the difference in the molecular weights of pure PA 6 and PA 6/PA 66 on the crystallization of PA 6 should be negligible. The presence of intermolecular interactions in a polymeric material significantly determines its morphological and structural properties. As for polyamides, the hydrogen-bonding ability gives rise to the crystalline structure of polyamides. This interaction is opposed to the trend to lower entropy that allows the polymer chains to align and display crystalline characteristics. In a linear conformation, the regularity can be greatest and allow maximum hydrogen-bonding interactions, giving minimum energy. This characteristic of hydrogen bonding allows polyamides to form stable intermolecular hydrogen bonds. It has been found[10] that even hydrogen bonding between molecules of polyamide and polyurethane is sufficiently strong to cause the polymer chains to distort rather than disrupt the hydrogen bonds. Because of the strong hydrogen bonding between PA 66 and PA 6 macromolecules, PA 66 could be molecularly incorporated into the PA 6 matrix through *in situ* polymerization. However, the different linear conformations of PA 66 and PA 6 macromolecular chains retard the greater regularity of PA 6 molecules and the optimization of hydrogen-bonding interactions. Thus, the weakening of hydrogen bonding in PA 6/PA 66 molecular composites leads to their decreasing crystallizability and more unstable crystalline structure, in comparison with those of pure PA 6.

Figure 3 shows the crystallization processes of pure PA 6 and PA 6/PA 66. The peak temperature at which the crystallization rate is maximum (T_c) and the crystallinity of the PA 6 composites decrease with an increase in the PA 66 concentration in PA 6/PA 66. The peak widths of PA 6/PA 66 are larger than that of pure PA 6, and this suggests that more incomplete crystallization occurs in PA 6/PA 66, in comparison with pure PA 6. All the results indicate that the intro-

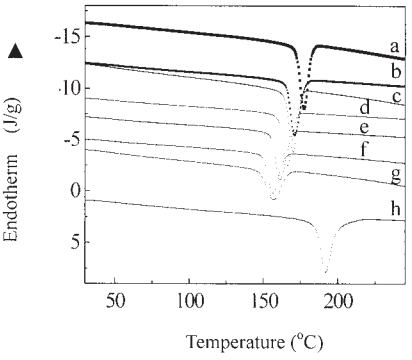

Figure 3 DSC crystallization curves of PA 6/PA 66 containing (a) 0 wt % PA 66, (b) 2 wt % PA 66, (c) 4 wt % PA 66, (d) 6 wt % PA 66, (e) 8 wt % PA 66, (f) 10 wt % PA 66, (g) 12 wt % PA 66, and (h) e-PA 6/PA 66 with 10 wt % PA 66.

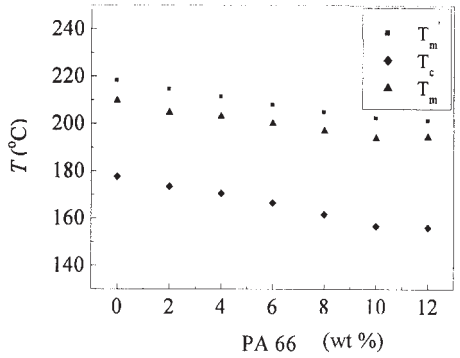

Figure 4 T_m, T_m', and T_c versus the weight percentage of PA 66 in PA 6/PA 66.

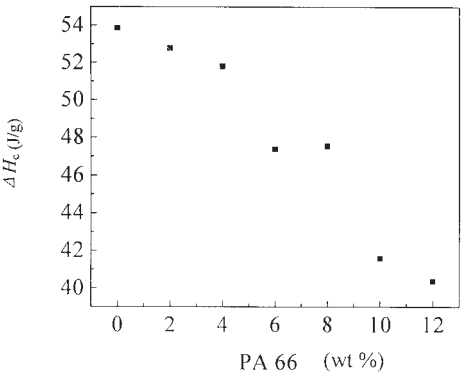

Figure 5 ΔH_c versus the weight percentage of PA 66 in PA 6/PA 66.

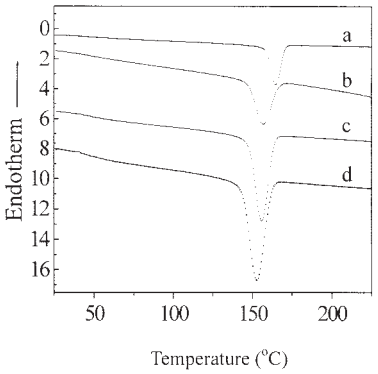

Figure 6 DSC crystallization curves of PA 6/PA 66 containing 12 wt % PA 66 at different cooling rates: (a) 5, (b) 10, (c) 15, and (d) 20°C/min.

duction of PA 66 into PA 6 retards the crystallization of PA 6 because of the good dispersion of PA 66 and the strong interactions between them.

The dependence of T_m, T_m', T_c, and the heat of crystallization (ΔH_c) on the various compositions of PA 66 is shown in Figures 4 and 5. With an increase in PA 66 (from 2 to 12 wt %), the T_m, T_m', and T_c values of PA 6 composites decrease in a linear form, and the slopes of these relationships are almost the same. Because of its inability to form its own crystallites and its homogeneous dispersion in the PA 6 matrix, one of the significant considerations in this case is the location of PA 66 macromolecules in the PA 6 matrix as a diluent. The diluent molecules can reside in the interspherulitic regions, interfibrillar regions, interlamellar regions, or some combination of these, yielding different microstructures, which in turn give rise to different material properties.[11–13] It has been proposed that the favorable intermolecular interactions gained by the mixing of the diluent with the amorphous phase of the crystalline polymer will promote interlamellar incorporation. The strong hydrogen bonding between PA 66 molecules and PA 6 molecules probably makes most PA 66 macromolecules incorporate in PA 6 interlamellar regions, and this leads to incomplete crystallization of PA 6, so the T_m, T_m', and T_c values of PA 6 composites decrease in proportion to the increase in the PA 66 concentration.

Figure 4 also shows that T_m' for the second scan is higher than T_m for the corresponding first scan. On the other hand, the difference of T_m and T_m' for the corresponding e-PA 6/PA 66 is less than 1°C. Therefore, it can probably be ascribed to incomplete crystallization under nonisothermal crystallization conditions in comparison with crystallization at the ambient temperature in the preparation of PA 6/PA 66.

ΔH_c of the PA composites decreases with the addition of PA 66, and ΔH_c decreases by approximately 10.5 J/g upon the addition of 12 wt % PA 66 (see Fig. 5). All the data again demonstrate that the crystallization of PA 6 is deeply disturbed by PA 66.

Kinetics of nonisothermal crystallization

Ozawa[14] extended the Avrami equation, originally valid for isothermal crystallization, to nonisothermal conditions by assuming that the sample is cooled at a constant rate and that the mathematical analysis proposed by Evans[15] is appropriate. Accordingly, the relative crystallinity [$X_{(T)}$], at temperature T and cooling rate R, is given by

$$1 - X_{(T)} = exp[-k_{(T)}/R^n] \quad (2)$$

where $k_{(T)}$ is the cooling function of nonisothermal crystallization at temperature T and n is the Ozawa exponent.

Figure 6 shows the crystallization exotherms for PA 6/PA 66 containing 12 wt % PA 66 at various cooling rates. T_c clearly moves to a low-temperature region with an increasing cooling rate.

From the DSC thermograms, the values of $X_{(T)}$ at different T_c values were calculated [shown in Fig. 7(a)], and a series of S-shaped curves were obtained. The relationship between T_c and the crystallization

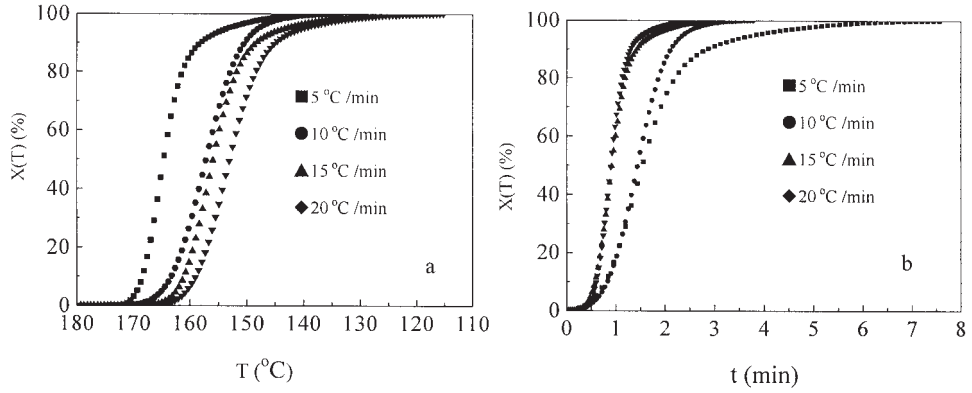

Figure 7 $X_{(T)}$ in the process of nonisothermal crystallization for PA 6/PA 66 containing 12 wt % PA 66: (a) T_c and (b) t.

TABLE II
Values of T_c, $t_{1/2}$, and ΔH_c in Nonisothermal Crystallization for Pure PA 6 and PA 6/PA 66 Containing 12 wt % PA 66

	Pure PA 6 at R (°C/min) of				PA 6/PA 66 at R (°C/min) of			
	5	10	15	20	5	10	15	20
T_c (°C)	183.83	177.59	173.1	172.4	165.11	157.08	156.19	153.2
$t_{1/2}$ (min)	1.3	0.8	0.35	0.35	1.5	1.4	0.85	0.85
ΔH_c (J/g)	64.44	50.86	52.93	53.62	50.03	40.37	47.51	47.04

time (t) is given by eq. (3) during the nonisothermal crystallization process:

$$t = [T_0 - T]/R \tag{3}$$

where T_0 is the initial temperature when crystallization begins ($t = 0$). The values of the X axis in Figure 7(a) can be transformed into t [shown in Fig. 7(b)]. Because of spherulitic impingement in the later stage, the curves tend to flatten and become S-shaped. The values of T and t at the various cooling rates and at random values of $X_{(T)}$ have been obtained from Figure 7. The half-time of nonisothermal crystallization ($t_{1/2}$), when $X_{(T)}$ is equal to 50%, have been acquired from Figure 7(b). The T_c, $t_{1/2}$, and ΔH_c values at different cooling rates are listed in Table II. The data indicate that for T_c, a very different dependence exists in the melt crystallization for the PA 6 composite. The $t_{1/2}$ data indicate that the higher the cooling rate is, the shorter the time is for crystallization completion. The values of $t_{1/2}$ of PA 6/PA 66 increase, in comparison with those of pure PA 6, and this again suggests that the introduction of PA 66 into the PA 6 matrix reduces the crystallization rate of PA 6 to some extent.

Equation (2) can be rewritten as follows:

$$\log[-\ln(1 - X_{(T)})] = \log k_{(T)} - n \log R \tag{4}$$

The calculated $X_{(T)}$ values have been analyzed according to eq. (3). The left side of eq. (3) has been plotted for a given temperature versus log R, as illustrated for the PA 6 composite with 12 wt % PA 66 in Figure 8. Because the spherulitic impingement occurs in the later stage, the curve fitting was only done for Y values lower than 0.36, corresponding to $X(T)$ values below 0.9. From Figure 8, a linear relationship is usually a good approximation in the higher T_c region (the primary stage, e.g., T_c = 160.0 and 162.5°C), so the Ozawa equation is applicable to the nonisothermal crystallization[15] of the sample in the primary stage. n (the primary stage) has been calculated from the slope of these straight lines.

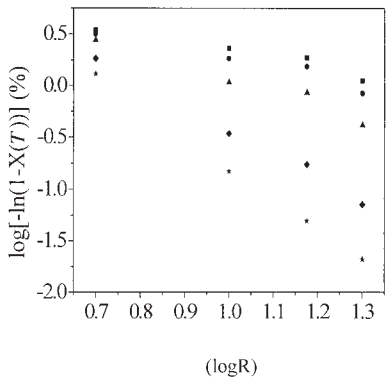

Figure 8 Plot of lg{−ln[1 − $X(T)$]} versus lg R during the nonisothermal crystallization process of PA 6/PA 66 containing 12 wt % PA 66: (■) 150, (●) 152.5, (▲) 155, (♦) 160, and (★) 162.5°C.

Table III indicates how n depends on the temperature. At 162.5°C, the value of n in PA 6/PA 66 is close to 3, which and this suggests that nucleation is heterogeneous, and the growth of spherulites is three-dimensional at the higher T_c (the primary stage). Because n decreases with the temperature, fractional values of n are observed, and this is usual for polymer crystallization [e.g., poly(vinylidene fluoride) (PVDF), polyethylene, polypropylene, PA 6, poly(ethylene terephthalate), and poly(ether ether ketone)].[16]

Fractional values of n have been explained by the dependence of the crystallization on the nucleation and growth mechanisms. At a constant growth dimension, n decreases by 1 when nucleation is heterogeneous rather than homogeneous. For the same nucleation mechanism, n increases with the growth dimension (e.g., from 1 for rods to 2 for disks and finally to 3 for spheres in the case of heterogeneous nucleation). It has been proposed that spherulites start to grow as rods; this happened for PVDF.[17] Moreover, Nandi[18] observed that the crystal morphology of PVDF was increasingly more disordered as T_c decreased. Therefore, a decrease in the crystallization growth dimension with the temperature seems to be a reasonable explanation for the data reported in Table III.

CONCLUSIONS

With the insertion of PA 66 into PA 6 at the molecular level, via *in situ* anionic polymerization, T_m and T_c of

TABLE III
***n* Values for Pure PA 6 and PA 6/PA 66 Containing 12 wt % PA 66 in the Primary Crystallization Process**

	Pure PA 6			PA 6/PA 66		
T	172.5	175	177.5	155	160	162.5
n	1.28	2.16	3.03	1.28	2.27	2.97

PA 6 in its composites with PA 66 decreased in a good linear relationship, and the crystallinities of the composites also decreased. The PA 6 composites had one melting temperature, whereas the coextruded PA 6/PA 66 blends had two melting temperatures; this suggested that PA 66 was more uniformly dispersed in the PA 6 composites than in the coextruded PA blends.

The data of the nonisothermal crystallization kinetics showed that $t_{1/2}$ increased for the PA 6/PA 66 molecular composite in comparison with that of pure PA 6, and this indicated that the crystallization rate of the PA 6/PA 66 composites was lower than that of pure PA 6. The values of n indicated that the nucleation was mainly heterogeneous in the primary stage. Generally, all the data indicated that the incorporation of PA 66 into PA 6 at the molecular level impeded the crystallization of PA 6.

References

1. Ou, Y. C.; Si, M. Y.; Yu, Z. Z. J Appl Polym Sci 1999, 73, 767.
2. Paul, D. R.; Newman, S. Polymer Blends; Academic: New York, 1999; Vol. 1, p 168.
3. Yu, L. L.; Yang, G. S. Macromol Rapid Commun 2004, 25, 1714.
4. Alfonso, G. C.; Chiappori, C.; Razore, S. In Reaction Injection Molding, Polymer Chemistry and Engineering; Kresta, J. E., Ed.; ACS Symposium Series 270; American Chemistry: Washington, DC, 1985.
5. Ueda, K.; Yamada, K.; Nakai, M.; Matsuda, T.; Hosoda, M.; Tai, K. Polym J 1996, 28, 446.
6. Ueda, K.; Nakai, M.; Hosoda, M.; Tai, K. Polym J 1996, 28, 1084.
7. Eersels, K. L. L.; Aerdts, A. M.; Groeninckx, G. Macromolecules 1996, 29, 1049.
8. Ho, J. C.; Wei, K. H. J Polym Sci Part B: Polym Phys 2000, 38, 2124.
9. Tomova, D.; Kressler, J.; Radusch, H.-J. Polymer 2000, 41, 7773.
10. Genovese, A.; Shanks, R. A. Comput Theor Polym Sci 2001, 11, 57.
11. Russell, T. P.; Stein, R. S. J Polym Sci Polym Phys Ed 1983, 21, 999.
12. Russell, T. P.; Ito, H.; Wignall, G. D. Macromolecules 1988, 21, 1703.
13. Zemel, J. P.; Zhang, X.; Miley, D. M.; Gullagher, K. P.; Zhang, A. Macromolecules 1992, 25, 3902.
14. Ozawa, T. Polymer 1971, 12, 150.
15. Evans, U. R. Trans Faraday Soc 1945, 41, 365.
16. Liu, Z. H.; Marechal, P.; Jerome, R. Polymer 1997, 38, 5149.
17. Keller, A. Makromol Chem 1959, 34, 1.
18. Nandi, A. K. Polymer 1994, 35, 5202.